

Supporting information for

Na₂Ru_{1-x}Mn_xO₃ as the Cathodes for Sodium-Ion Batteries

Xiang Li,^{a, b, c} Shaohua Guo,^{a, c*} Feilong Qiu,^a Linlin Wang,^d Masayoshi Ishida^b and Haoshen Zhou^{a, b, c*}

a. Center of Energy Storage Materials & Technology, College of Engineering and Applied Sciences, National Laboratory of Solid State Microstructures, and Collaborative Innovation Center of Advanced Microstructure, Jiangsu Key Laboratory of Artificial Functional Materials, Nanjing University, Nanjing 210093, China.

b. Graduate School of System and Information Engineering, University of Tsukuba, Tennoudai 1-1-1, Tsukuba, 305-8573, Japan

c. Energy Technology Research Institute, National Institute of Advanced Industrial Science and Technology (AIST), Japan.

d. Nanjing Univ, Sch Chem & Chem Engn, Collaborat Innovat Ctr Chem Life Sci, State Key Lab Analyt Chem Life Sci, Nanjing 210093, Jiangsu, Peoples R China

Experimental procedure

Synthesis of $\text{Na}_2\text{Ru}_{1-x}\text{Mn}_x\text{O}_3$

The $\text{Na}_2\text{Ru}_{1-x}\text{Mn}_x\text{O}_3$ compounds were prepared by solid state method. A stoichiometric ratio of Na_2CO_3 (5% excess for any evaporative sodium loss at high temperature), RuO_2 and MnO_2 were used as the raw materials. The mixture was ground in an agate mortar with a pestle for homogeneity and was then pressed into pellets. The pellets were heated at 700 °C for 2h and 850 °C for 12 h in Ar atmosphere. The heating rate was maintained at 5 °C min⁻¹.

Structural and electrochemical characterizations

The compounds were characterized by powder X-ray diffraction (XRD) on a Bruker D8 Advance diffractometer using $\text{CuK}\alpha$ radiation (40 kV and 40 mA) with a scanning speed of 0.5 min⁻¹ in steps of 0.02°.

The electrochemical measurements of the compounds were examined by 2032 type coin cells, and sodium metal served as counter electrode with a glass fiber film as separator. The samples (80%) were mixed with 10% AB carbon black (acetylene black) and 10% PTFE (polytetrafluoroethylene) binder as a positive electrode. The electrode was pressed on aluminium foil substrate, and then dried under vacuum at about 110 °C overnight and transferred to a glove box under Ar atmosphere before cell assembly. The electrolyte was 1 M NaPF_6 in EC (ethylene carbonate) and DEC (diethyl carbonate). The galvanostatic charge-discharge tests were performed by using a Hokuto Denko HJ1001SD8 battery tester at different current densities at 25 °C after a rest for 8 h.

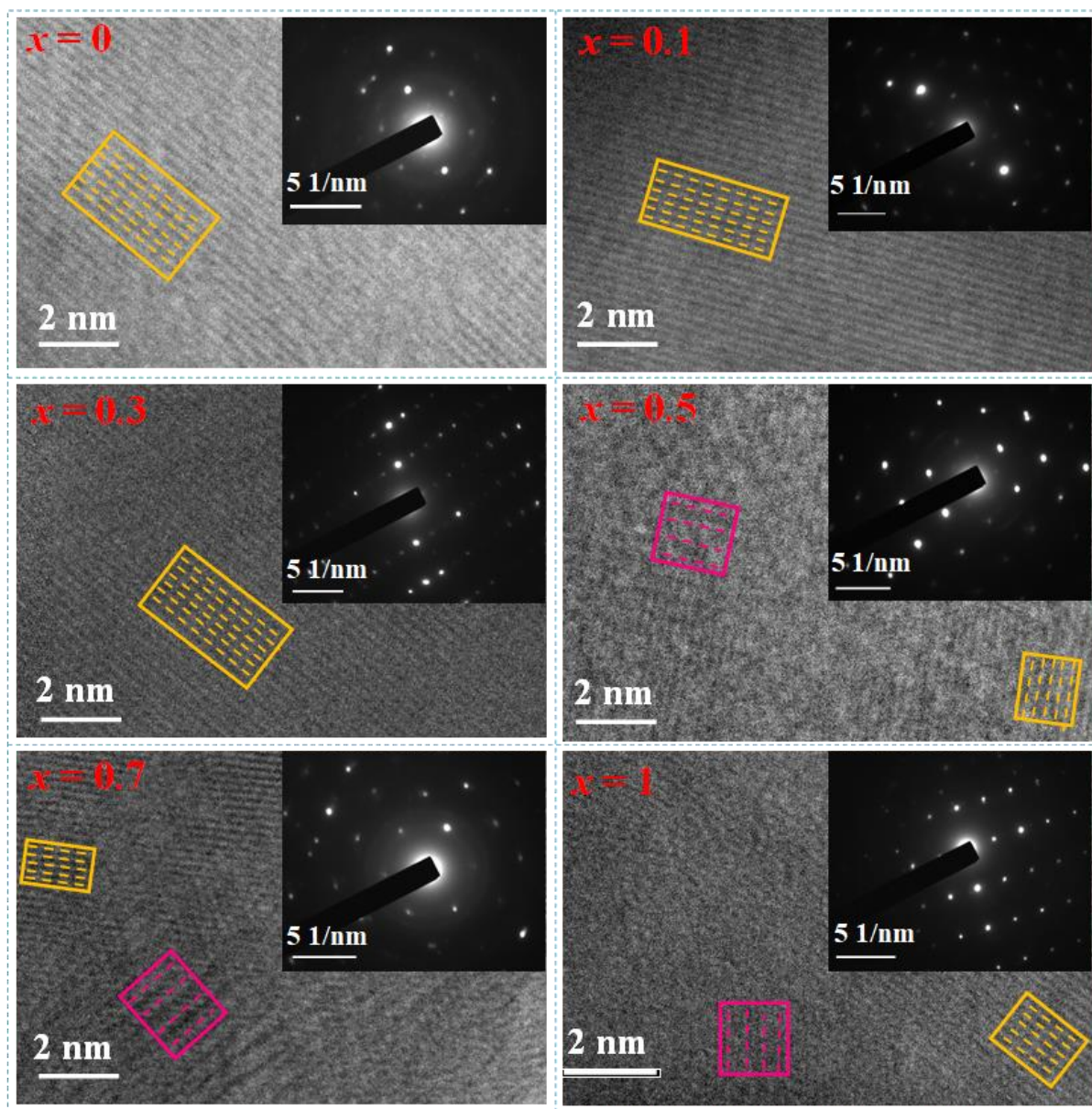


Figure S1. TEM images of different $\text{Na}_2\text{Ru}_{1-x}\text{Mn}_x\text{O}_3$ with corresponding selected area electron-diffraction pattern.

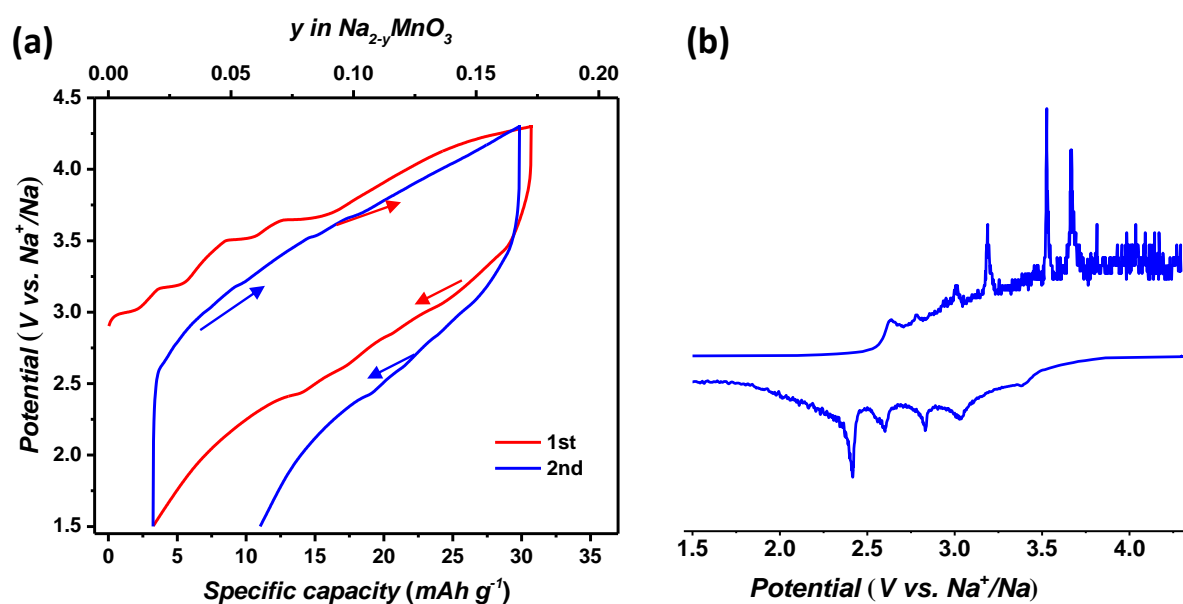


Figure S2. (a) The typical galvanostatic potential curves of Na_2MnO_3 for the initial two cycles at the current density of 10 mA g^{-1} . (b) The corresponding dQ/dV curves with the second cycle derived from (a).

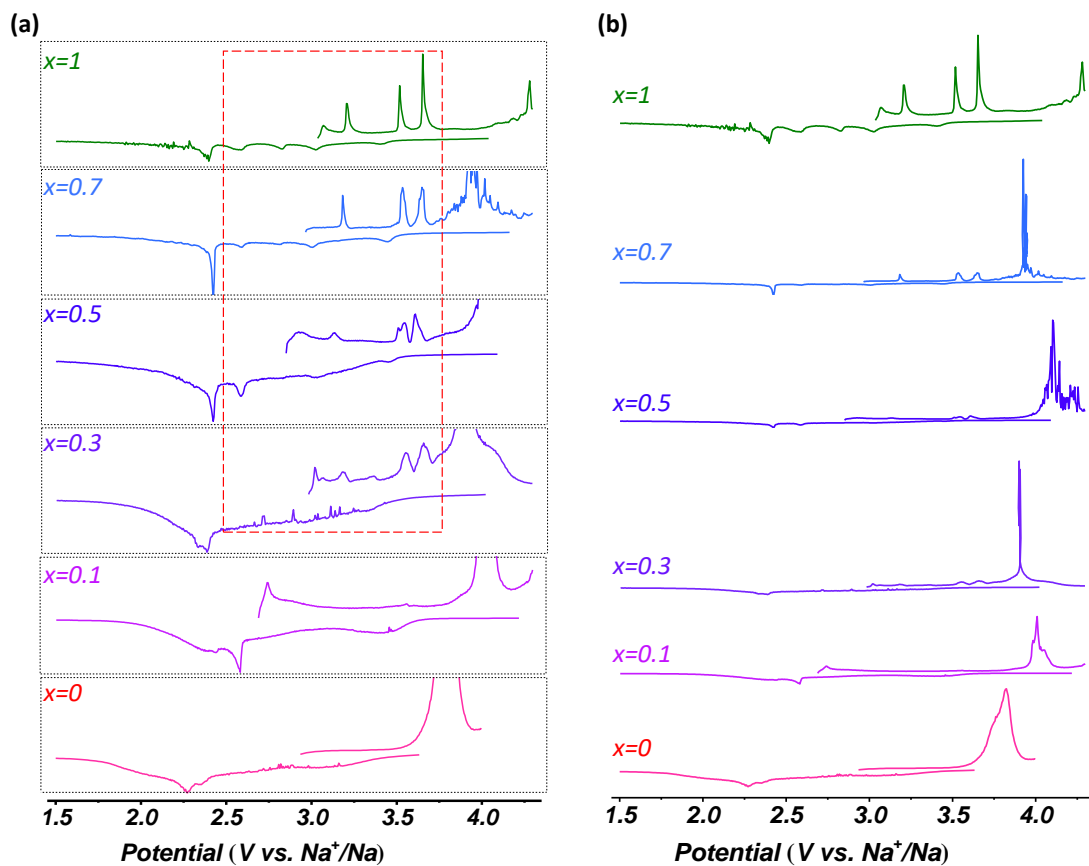


Figure S3. The corresponding dQ/dV curves of the first cycle derived from Figure 2a. Figure S3a is enlarged from Figure S3b.

It is clear that when x is larger than 0.1, there appear additional peaks during the first charging process. The peaks are highlighted by the dot red rectangle. These peaks indicate undesired phase transitions which will deteriorate the structural stability and therefore destroy the cycling performance

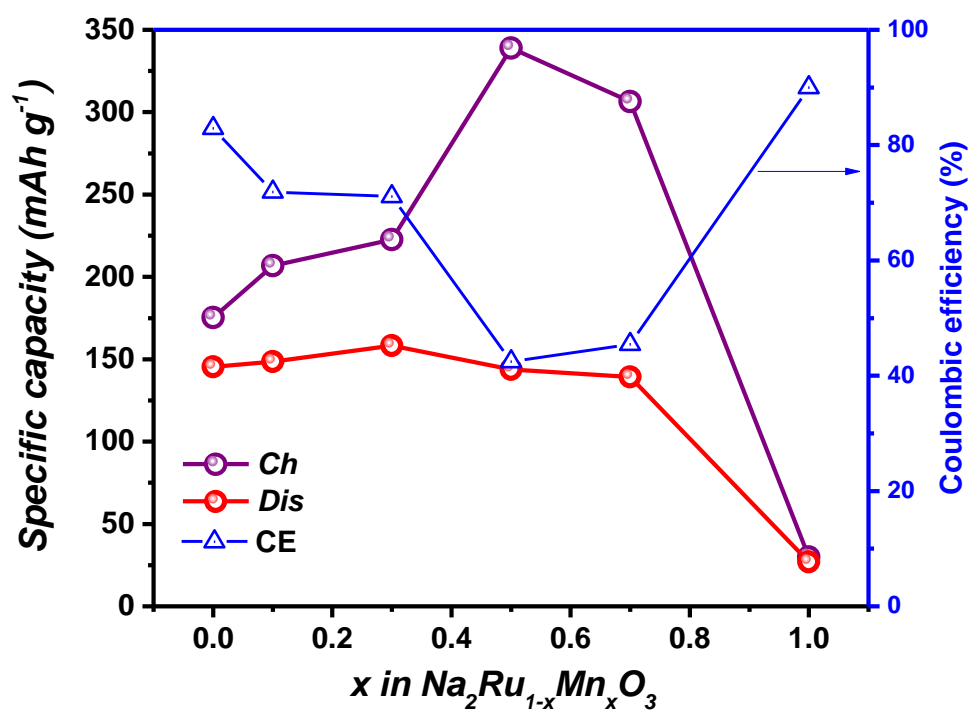


Figure S4. The comparison of different $\text{Na}_2\text{Ru}_{1-x}\text{Mn}_x\text{O}_3$ with charge capacity, discharge capacity and coulombic efficiency for the first cycle at the current density of 10 mA g^{-1} .

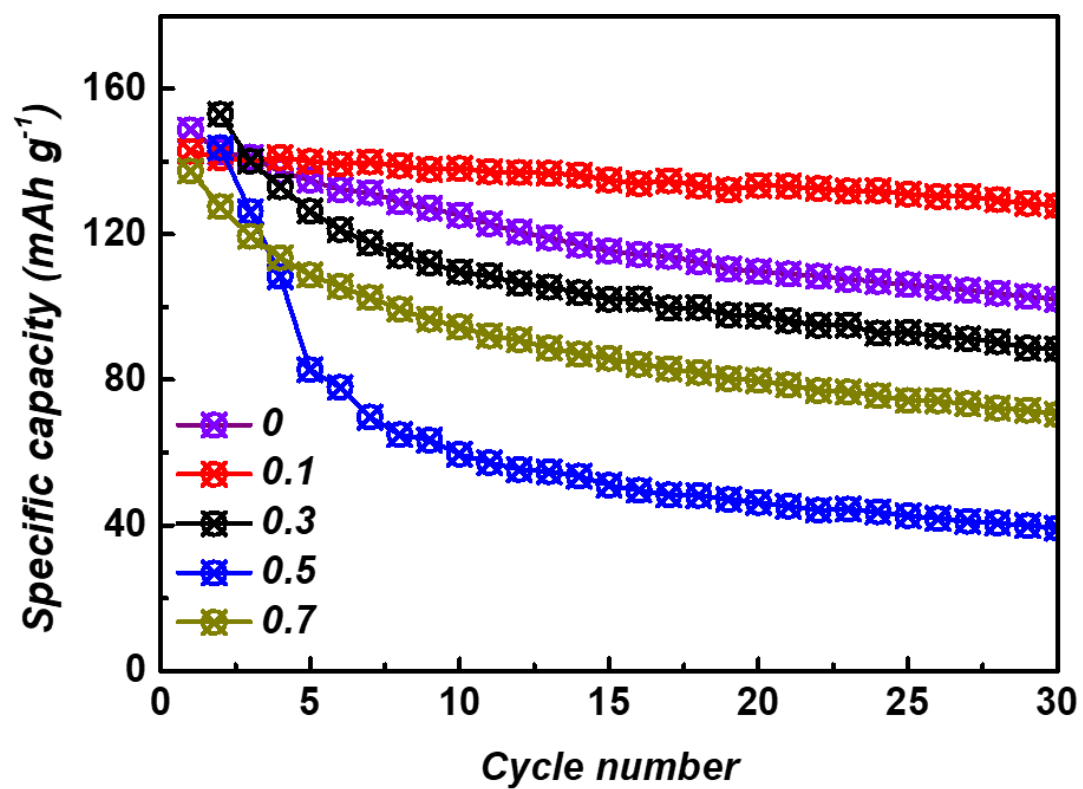


Figure S5. The cycling performance for different Na₂Ru_{1-x}Mn_xO₃ at the current density of 20 mA g⁻¹.

Table S6. The resistances of different cathodes of $\text{Na}_2\text{Ru}_{1-x}\text{Mn}_x\text{O}_3$ by using 4-point conductivity.

Samples	R1 (R = resistance, $\text{K}\Omega$)	R2 ($\text{K}\Omega$)	R3 ($\text{K}\Omega$)
$x = 0$	0.6	0.7	0.6
$x = 0.1$	0.5	0.5	0.6
$x = 0.3$	1.1	0.8	0.7
$x = 0.5$	0.8	1.0	1.0
$x = 0.7$	0.7	0.6	0.6
$x = 1$	0.9	0.8	1.0

The cathodes are ~ 1 mg with a diameter of 7 mm. Each electrode was tested for three times.

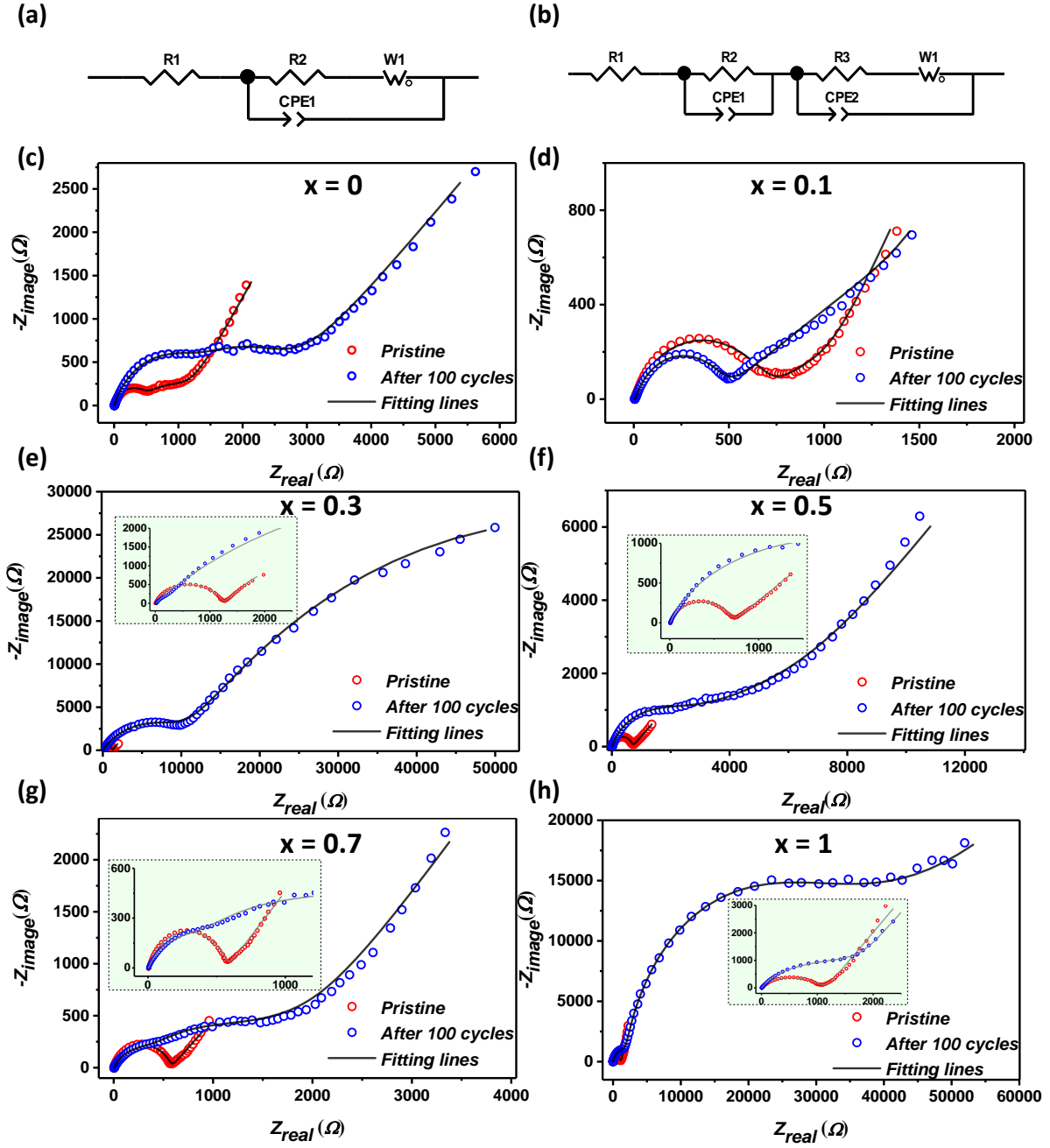


Figure S7. (a) Equivalent circuit for fitting the pristine cells. (b) Equivalent circuit for fitting the cells after 100 cycles. EIS curves of $\text{Na}_2\text{Ru}_{1-x}\text{Mn}_x\text{O}_3$ for the pristine cell and cell after 100 cycles with fitting. (c)-(h) represents $x = 0$, $x = 0.1$, $x = 0.3$, $x = 0.5$, $x = 0.7$ and $x = 1$ respectively. Insert figures are amplified for comparison.

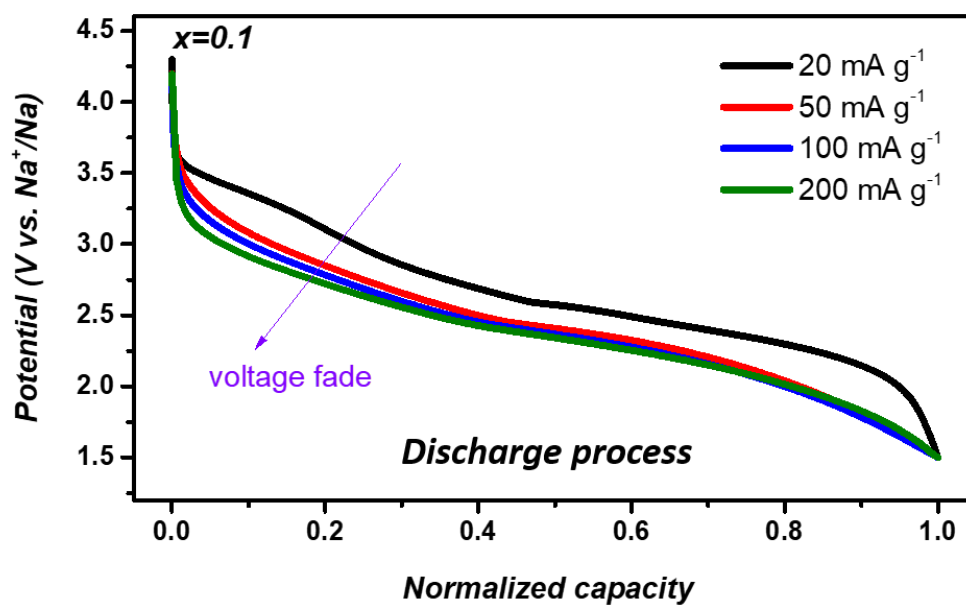


Figure S8. The discharge curves based on normalized capacity for the sample $x = 0.1$ with different current densities.

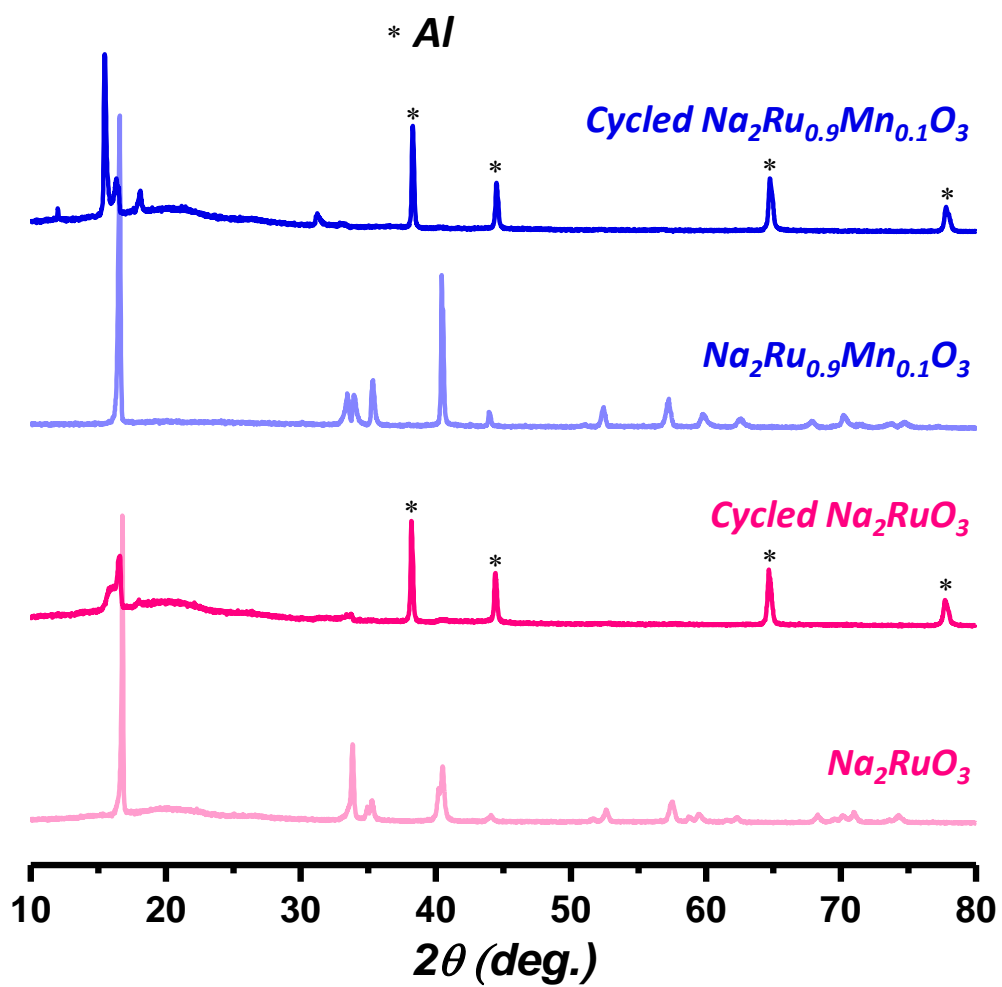


Figure S9. Ex-situ XRD patterns of pristine Na_2RuO_3 and $\text{Na}_2\text{Ru}_{0.9}\text{Mn}_{0.1}\text{O}_3$, compared with the cycled Na_2RuO_3 and $\text{Na}_2\text{Ru}_{0.9}\text{Mn}_{0.1}\text{O}_3$ after 100 cycles at the current density of 100 mA g^{-1} .

Table S10. Electrochemical performance of different TM-doped Na₂RuO₃ in sodium half-cells.

Sample	Na₂Ru_{0.95}Zr_{0.05}O₃	Na₂Ru_{0.75}Sn_{0.25}O₃	Na₂Ru_{0.9}Mn_{0.1}O₃
Cycle life (cycles)	200	50	100
Current density (mA g ⁻¹)	136	7	100
Potential window (V)	1.5-3.5	1.5-4.2	1.5-4.3
Capacity of 1 st cycle	136 mAh g ⁻¹	140 mAh g ⁻¹	~150 mAh g⁻¹
Capacity retention	77 %	71 %	76 %
Ref.	1	2	This work

References

1. S. Song, M. Kotobuki, F. Zheng, Q. Li, C. Xu, Y. Wang, W. D. Z. Li, N. Hu and L. Lu, *J. Power Sources*, 2017, 342, 685.
2. P. Rozier, M. Sathiya, A.-R. Paulraj, D. Foix, T. Desautay, P.-L. Taberna, P. Simon and J.-M. Tarascon, *Electrochem. Commun.*, 2015, 53, 29.